TAUP 1560-87

Detection of New Particles Produced in $\gamma\gamma$ Collisions with OPAL at LEP

C. Milstène

School of Physics and Astronomy
Tel-Aviv University , Tel-Aviv, Israel

I. Introduction

In e^+ e^- collisions at LEP energies the 2γ processes are one of the dominant reactions (fig.1). The cross-section $\sigma(e^+ e^- \xrightarrow{\gamma\gamma} e^+ e^- X)$ is proportional to $\ln^2(s)$ and is of the order of 30 nb at E_{cm} = 100 GeV. For an integrated luminosity of 500 pb^{-1} one expects therefore a total of 30 x 5 10^5 = 1.5 10^7 two-photons events in the range of $W = W_{\gamma\gamma}$ = 1-99 GeV. Even in the range of energy $W_{\gamma\gamma}$ = 50±0.5 GeV, the number of events produced will reach approximately 10^5 events and thus is attractive for the search of new particles in 2γ collisions.

To study the feasibility of the OPAL detector at LEP I to search for new particles in $\gamma\gamma$ collisions, we consider the reaction $\gamma\gamma \rightarrow$ Resonance induced by 50 GeV incoming electron-positron colliding beams. We assume a Breit-Wigner behavior of the cross section [1]

$$\sigma = (2J+1)\ 8\pi K\ (W/M_R)\ \frac{\Gamma_{tot}\Gamma_{\gamma\gamma}}{(W^2-M_R^2)^2+(\Gamma_{tot}\ M_R)^2}$$

for a particle with a spin J and a mass M_R. Here $K=0.38938 \cdot 10^6$ is the conversion constant from GeV^{-2} to nb. The total width of the resonance is Γ_{tot} and its partial width to $\gamma\gamma$ is $\Gamma_{\gamma\gamma}$. One can see that at the peak, the cross-section varies as $\Gamma_{\gamma\gamma}/(\Gamma_{tot}M_R^2)$, but the integrated cross-section which is proportional to the number of events under the resonance, is essentially independent of Γ_{tot} [2]. In this note we discuss the formation of new massive particles in $\gamma\gamma$ collisions, the masses considered are M_R= 20, 30, 40 and 50 GeV, with a spin J=0, having a $\Gamma_{\gamma\gamma}$ in the vicinity of 10 MeV and decaying either into 2 jets or into 2γ.

One should note that classes of new particles with comparable masses and $\Gamma_{\gamma\gamma}$ in the range 5 to 70 GeV have been previously theoretically discussed [3].

In section II we will introduce the methods of calculations for both the new parti-

cles signals and their background. The particles decaying into 2 jets and their background will be treated separately and then the particles decaying into 2γ and their background will be studied. In section III we will deal in detail with the background to a resonance produced in 2γ and decaying into 2 jets, namely the background from $e^+ e^-$ - 1γ - annihilation produced in the Z° region using the Lund programs [4] and the 2γ background. The production of the resonance particles decaying into 2 jets will be described in section IV. The predictions for the standard Higgs with a mass dependent $\Gamma_{\gamma\gamma}$ of the order of 0.5 keV and a Γ_{tot} of the order of 1 MeV [5] and the supersymmetric extension of the standard model with enhanced Higgs [6], will be considered in the same section. In the next two sections the predictions for the particles signal, decaying into 2γ and their background will be considered. The background to such events is studied in section V and the signal in section VI. The signal is obtained by simulation with a Monte-Carlo program and $\Gamma_{\gamma\gamma}$ of the order of 10 MeV. Here the predictions of compositeness for the pseudo-Goldstone boson [6] are used as our signal.

Finally in section VII we conclude with an estimate of the minimum $\Gamma_{\gamma\gamma}$ needed for a resonance detection.

II Method of calculation

The calculations are carried out in two steps for the 2γ collisions using software programs which were first developed for the PETRA detectors. The OPAL detector was simulated by fast simulation DETECO program, written for ELECTRA and implemented to fit OPAL. The 2 steps are a) and b):

a) $e^+ e^- \rightarrow e^+ e^- \gamma\gamma$, $\gamma\gamma \rightarrow$ hadrons, which is the product of 2 amplitudes:

Amplitude(QED) • Amplitude($\gamma\gamma \rightarrow$ hadrons)

The Amplitude(QED) is the Luminosity function assuming transverse polarized photons in the process $e^+ e^- \rightarrow e^+ e^- \gamma_T \gamma_T$ [7]. The W dependence of the process $\gamma\gamma \rightarrow$ hadrons in the resonance is the Breit-Wigner given above. For the background the W dependence is given by the expression $\sigma = A+B/W_{\gamma\gamma}$ [8].

b) The production of the resonance and its fragmentation into 2 jets, isotropically distributed around the $\gamma\gamma$ axis, is taken care of by using a Lund program developed for PETRA.

The momentum distribution of the particles in the background is obtained from the limited p_T phase space, with an $\exp(-a\, p^2_T)$ distribution taking a=5 .

III The background to particles decaying into 2 jets

The number of events from the background obtained for an integrated luminosity of L = 500 pb^{-1} is given in Table I. In the expression of $\sigma = A+B/W_{\gamma\gamma}$ we have used A=253 nb and B=695 nb-GeV [8]. For each mass the background will be summed up in the same range of detected visible energy W_{vis} as the resonance. These energy background bins have been chosen to match the W_{vis} range obtained from the 2-jets decay of the resonance under study. In fig. 2 an example of a W_{vis} distribution for a resonance at M_R= 50 GeV, is given, as one can see it is contained mainly between W_{vis} of 44 and 52 GeV. Note that the W_{vis} range is not symmetrical around the resonance mass value.

Table I

Expected background events from $\gamma\gamma$ and 1γ annihilations

	$\gamma\gamma$ Background		1γ annihilation background
M_R (GeV)	W_{vis} range (GeV)	# events	# events
20	14-22	$4.20\ 10^5$	$8.7\ 10^3$
30	24-32	$1.76\ 10^5$	$1.2\ 10^4$
40	34-42	$1.06\ 10^5$	$2.0\ 10^4$
50	44-52	$6.04\ 10^4$	$6.8\ 10^4$

For the $\gamma\gamma$ background, we have chosen to sum up all contributions of the W values in the range from 1 to 99 GeV. We have checked that the number of events under the resonance is only slightly sensitive to our choice of the lower W limit. For example, for the range 10 to 99 GeV we get $6\ 10^4$ events for M_R = 50 GeV instead of $6.8\ 10^4$ events in the range 1 to 99 GeV.

The number of background events coming from $e^+ e^-$ - 1γ - annihilation is presented in fig. 3a for the OPAL detector with an angular acceptance of 97% of

4π. One notices that these events are concentrated mostly above 66 GeV with a peak at about 92 GeV. This concentration at high W_{vis} energies is advantageous for study of resonances at relatively lower masses. In order to show the importance of a 4π geometry detector we also present in fig. 3b the correspondent W_{vis} distribution for a detector with only a 64% of 4π angular acceptance for charged particles. As can be seen, the effect of a lower acceptance produces a much longer tail toward lower W_{vis}. This would be a serious handicap in the detection of resonances produced in $\gamma\gamma$ collisions down to $M_R \simeq 20$ GeV.

IV. Resonances decaying into 2 jets

We will present below the expected number of events for a J=0 resonance having a width $\Gamma_{\gamma\gamma} = 10$ MeV and decaying into 2 jets. The number of events obtained for an integrated luminosity of 500 pb^{-1} assuming the masses values M_R = 20, 30, 40 and 50 GeV are represented in Table II. The events were counted within the visible energies of $(M_R + 2)$ GeV and $(M_R - 8)$ GeV as implied from the Monte-Carlo distributions obtained and an example of which, is shown in fig. 2 for $M_R = 50$ GeV.

We have considered three different cuts which should suppress the background and therefore improve the detection efficiency of the signal. The first one concerns the charge multiplicity, the second the Thrust axis angular distribution and the third the missing p_T of the event.

A distribution of the charged multiplicities after detection is shown in fig. 4a, for the 2γ background and in fig. 4b for the signal. A comparison of those distributions shows that the background is rich in small charged multiplicity ,smaller than 4 prongs, whereas those low charged multiplicities events are sparse for the signal. A cut at a charged multiplicity $n_{ch} = 4$ is performed.

The distributions of the polar angle cosΘ of the Thrust axis with respect to the beam direction is shown fig. 5. One can see an enhancement for $ABS(\cos\Theta_{Thrust}) \geq 0.9$ for the 2γ background (fig. 5a). The same kind of enhancement is seen in the 1γ annihilation distribution in fig. 5b for high values of ABS(cosΘ). The same distribution for the signal is almost flat. This distribution is shown in fig. 5c for the signal at 50 GeV, from which we have chosen the cut $ABS(\cos\Theta) \geq 0.9$.

The distribution of the missing p_T is also considered. In fig. 6a one can see that

the 1γ annihilation background after detection has a longer tail at the higher missing p_T. A comparison to the same distribution for a resonance at 50 GeV, given in fig. 6b, shows that a cut performed at a missing $p_T \geq 5$ GeV allows to eliminate part of the annihilation background.

In Table II the number of events before and after the cuts are shown together with the total background (sum of the 1γ and 2γ background) before and after those cuts. One obtains for example that the signal to background at 40 GeV is improved from 8 standard deviations to 19 standard deviations. Thus we can detect resonances with either a BR (R→hadrons) or a $\Gamma_{\gamma\gamma}$ smaller by a factor 4 than without cuts.

Table II

No. of non-standard Higgs events in $\gamma\gamma$ collisions
and the expected total background events, with and without cuts.

Before cuts					After cuts		
M_R (GeV)	W_{vis} (GeV)	# BG Evts from $1\gamma+2\gamma$	# Evts signal	s.d.	# BG Evts from $1\gamma+2\gamma$	# Evts signal	s.d.
20	14-22	$4.29\ 10^5$	$7.06\ 10^4$	108	$2.96\ 10^4$	$5.60\ 10^4$	326
30	24-32	$1.88\ 10^5$	$1.10\ 10^4$	25	$2.14\ 10^4$	$9.51\ 10^3$	65
40	34-42	$1.26\ 10^5$	$2.77\ 10^3$	8	$1.76\ 10^4$	$2.45\ 10^3$	19
50	44-52	$1.28\ 10^5$	$0.87\ 10^3$	2.4	$2.39\ 10^4$	$0.77\ 10^3$	5

One notices that the total background decreases from 20 GeV to 40 GeV and increases again at 50 GeV due to the contribution of the 1γ annihilation background coming from the region of the Z°. The contribution of the 1γ annihilation background ,which was almost one order of magnitude smaller than the 2γ background in the whole range below 50 GeV, becomes comparable to it at this energy and increases up to 100 GeV. In evaluating the results given in Table II one should notice, however, that the W_{vis} distribution of background behaves smoothly with energy in

the range of interest here. Thus the detection sensitivity for new resonances will depend to the first approximation on the square root of the number of background events under the resonances. Hence, for example, at 20 GeV the statistical error on the total background after cuts is 172 events whereas the resonance contains 56000 events which can comfortably be detected above the total background. In fact even a resonance with 1/65 of the actual signal, i.e. 860 events (5 standard deviations) is still measurable. This allows the detection of a resonance with either a BR (R $\rightarrow$ hadrons) > 1/65 or a $\Gamma_{\gamma\gamma}$ value smaller by a factor 65 than expected for the 10 MeV resonance studied, or any combination of the partial width reduction and BR reduction which ends-up to a factor 65 smaller. If we perform only a width reduction, one sees than in order to get 5 standard deviations above the background after cuts when M_R = 20, 30, 40 GeV , the minimal partial width of the resonances is $\Gamma_{\gamma\gamma}$ = 0.15, 0.77, 2.6 MeV, whereas at M_R = 50 GeV the width of 10 MeV is the minimal width already.

We will now study the case where the new particle is the standard Higgs. As mentioned in section I the number of events in the resonance peak is proportional to the ratio $\Gamma_{\gamma\gamma}/(\Gamma_{tot}\ M_R^2)$. In this case we get from ref. 5 that :

$\Gamma_{tot} = (G_F/\sqrt{2})\ (m_b^2/4\pi)\ m_H$, with the mass of the b quark m_b = 5 GeV, so that Γ_{tot} is varying for M_R = 20 to 50 GeV respectively from 0.2 MeV to 0.8 MeV. Here we have taken a Γ_{tot} of 1 MeV since the result is almost independent of Γ_{tot} for the resolution of OPAL as mentioned in section I (see also [2]). The partial width :

$\Gamma_{\gamma\gamma} = (\alpha^2 / 8\sqrt{2}\pi^3)\ G_F\ M_H^3\ I^2$ and $I = I_{leptons} + I_{Hadrons} + I_W$, where according to ref. 5 for massive Higgs, the values of $I_{hadrons}$, $I_{leptons} \rightarrow 0$ and only W contributes via the triangle diagram (see fig.4), with $I_W = -(7/4)$. One can see from the expression for $\Gamma_{\gamma\gamma}$ that the partial width to $\gamma\gamma$ for the standard Higgs is proportional to the third power of the mass of the Higgs. Hence one obtains for M_R = 20, 30, 40 and 50 GeV the values of $\Gamma_{\gamma\gamma}$= 0.05, 0.15, 0.35 and 0.70 keV respectively to compare with the value of $\Gamma_{\gamma\gamma}$= 10 MeV assumed in our calculations. The number of events in the signal will therefore be a factor 10^4 to 10^5 times smaller than in our calculations above and displayed in Table II. We can therefore conclude that the number of events expected for a standard Higgs in the $\gamma\gamma$ reactions is hopelessly small and highly superseded by the background.

The supersymmetric models mentioned in [6], however, predict an enhanced Higgs which might be detected. We will present below the predictions of the supersymmetric extension of the standard Higgs assuming a dominant two jets decay mode. In the non-standard SUSY extension of GSW there are 8 degrees of freedom, 3 of them serve to give masses to $W^{\pm}$ and Z°, and instead of one neutral scalar physical Higgs H° we get 5 Higgses including 2 charged ones [6], H°, S°, P°, $S^{\pm}$.
The Yukawa coupling includes 2 additional parameters, the H°-S° mixing angle Θ and the ratio of 2 vacuum expectation values tg(α), which is not fixed by the model. For ABS(tg(α)) >> 1 there is a dramatic enhancement factor X_f where f= u,d,lepton, which increases the partial width $\Gamma_{\gamma\gamma}$, namely :

$$\frac{\Gamma_{\gamma\gamma}}{M^3_{S_o}} = (G.S.W)_{Fermionic} \cdot X_f^{\,2}$$

Furthermore, all charged heavy SUSY partners ($\tilde{q}$,$\tilde{l}$) contributes via the triangle diagram given in fig. 7. An enhancement $X_l = X_d >> 1$ will be favorable to $\gamma\gamma$ collisions. This enhancement factor can even reach a value $X_l = X_d = 130$. The enhancement effect is illustrated in fig. 8 (taken from ref. 6), where one can see the predictions for $(\Gamma_{\gamma\gamma} \cdot BR)/(M_R^3)$, for the different $\Gamma_{\gamma\gamma}$ ranges of the GSW Higgs and the non-standard u,d enhanced Higgs. In the same figure the author of ref. 6 also shows for comparison the composite scalar X° to lower limits at PETRA/PEP and LEP. The region above the limits corresponds to more than 20 events at an assumed integrated luminosity of 100 pb^{-1} for PETRA/PEP and 20 pb^{-1} at LEP. Note that here we consider for LEP an integrated luminosity of 500 pb^{-1} which will increase the sensitivity of the experiment by a large factor.
Using the partial width $\Gamma_{\gamma\gamma}$ enhancement given by ref. 6 and shown here in fig. 8 one gets for the d enhancement Higgs a factor 10^3 above that of the standard Higgs. Hence for M_R =20,30,40 and 50 GeV we get $\Gamma_{\gamma\gamma}$ = 0.05, 0.15, 0.35 and 0.70 MeV which are not too far away from the minimum detectable values of $\Gamma_{\gamma\gamma}$ = 0.15, 0.77, 2.6 and 10 MeV after cuts corresponding to a 5 standard deviations effect.

V. Background to the 2γ decay channel

Here we will consider the pseudo-Goldstone boson as predicted in [6], choosing again for its mass the values M_R = 20, 30, 40 and 50 GeV but decaying now only into 2γ states. For this particular study, we will confine ourself to an approximate computation of the background rather than make use of an extensive Monte-Carlo

simulation.

The contribution of the radiative $e^+ e^-$ annihilation into 2γ, after emission of a forward bremsstrahlung γ from one (or both) of the beam particles is schematically represented in the diagram fig. 9. In the following we assume that if only 2 photons are seen in the detector, then the undetected photon is the bremsstrahlung one. This process may decrease the energy of the $W_{\gamma\gamma}$ system below 100 GeV (twice the beam energy) to the values of M_R considered above, so that it will fake our 2γ "true events".

From simple kinematics, we know that in order to leave the $e^+ e^-$ system in the appropriate energy region around M_R, the bremsstrahlung γ has to be produced within the energy range given by: $E_\gamma = \frac{4E_e^2 - (M_R + \Delta M)^2}{4E_e}$. For the analysis we have taken ΔM=1 GeV to guarantee that the radiative $e^+ e^-$ center of mass system lies within the resonance mass, e.g. a bremsstrahlung γ in the energy range $[E_{\gamma 1}, E_{\gamma 2}] = [45.2 \text{ GeV}, 45.8 \text{ GeV}]$, the two other γ will have an invariant mass $M_R = 30 \pm 1$ GeV. We will make a rough estimate of P_{brem}, which is the probability that the bremsstrahlung γ to be in the range of $[E_{\gamma 1}, E_{\gamma 2}]$, which corresponds to a resonance with a mass M_R according to the formula above. This is given by the expression :

$$P_{brem} = \left(\int_{E_{\gamma 1}}^{E_{\gamma 2}} dE_\gamma / E_\gamma \right) / \left(\int_{E_{\gamma_o}}^{50} dE_\gamma / E_\gamma \right)$$

where E_{γ_o} is the lower cutoff determined by the experimental sensitivity. This probability depends only slightly on the lower value E_{γ_o} e.g. for the values of $E_{\gamma_o} = 0.1$ and 0.5 GeV the normalization integral varies only from 6.2 to 4.6, here we have chosen $E_{\gamma o} = 0.1$ GeV for our computations. In this way the number of $e^+ e^- \to \gamma\gamma\gamma$ events is given by :

$$N = 2 \cdot P_{Brem} \cdot \sigma^o(e^+ e^- \to (\gamma\gamma)_{M_R}) \cdot \text{Luminosity}$$

where σ^o is the cross-section of $e^+ e^- \to \gamma\gamma$ after emission of a bremsstrahlung γ which is given in ref. 9 by $\sigma^o = K \frac{2\pi\alpha^2}{M_R^2} \left(\ln\left(\frac{M_R^2}{m_e^2} \right) - 1 \right)$

where K is the conversion factor from GeV^{-2} to nb. The factor 2 takes into account the fact that both e^+ and e^- may radiate.

The number of events obtained for the various masses are given in Table III, where one can see that they decrease smoothly from $8.6\ 10^3$ to $4.9\ 10^3$ as M_R increases from 20 to 50 GeV.

Table III

Expected background events from $e + e^- \rightarrow (\gamma_{brem})\ \gamma\gamma$

M_R (GeV)	W_{vis} range (GeV)	$E_{\gamma range}$ of brem. γ (GeV)	P_{brem}	σ_0 (nb)	# events
20	16-22	47.8-48.2	$2.6\ 10^{-3}$	6.6	$8.6\ 10^3$
30	26-32	45.2-45.8	$4.3\ 10^{-3}$	3.1	$6.5\ 10^3$
40	36-42	41.6-42.4	$6.0\ 10^{-3}$	1.89	$5.7\ 10^3$
50	46-52	37-38	$8.6\ 10^{-3}$	1.15	$4.9\ 10^3$

We will next consider the background coming from the 2γ collisions, $\gamma\gamma \rightarrow \pi^\circ\ \pi^\circ$.

For this we assume that the total hadrons multiplicity is given by a Poisson distribution. From this one can compute the probability to have 2 charged pions, which is twice the probability of having $2\pi^\circ$. The results of this calculation are given in Table IV together with the total multiplicity $N_{tot} = N_{charged} + N_{neutral}$, taken from the Lund Monte Carlo. One sees that the background under the resonances is negligible and decreases from 2 to $1.0\ 10^{-5}$ events for M_R = 20 to 50 GeV respectively.

Table IV

Expected background $\gamma\gamma \to \pi^0\ \pi^0$ and $\pi^+\ \pi^-\ \pi^0\ \pi^0$

M_R (GeV)	$\langle N_{tot} \rangle$	$P_{2\pi^0}$	# events	$P_{\pi^+\ \pi^- 2\pi^0}$	# events
20	17	$3.0\ 10^{-6}$	2.0	$1.5\ 10^{-4}$	$1\ 10^{-1}$
30	20	$2.1\ 10^{-7}$	$4.0\ 10^{-2}$	$1.4\ 10^{-5}$	$5\ 10^{-4}$
40	23	$1.4\ 10^{-8}$	$2.0\ 10^{-3}$	$1.2\ 10^{-5}$	$2\ 10^{-4}$
50	27	$3.5\ 10^{-10}$	$1.0\ 10^{-5}$	$3.5\ 10^{-8}$	$3\ 10^{-6}$

Another background which was considered is coming from $\gamma\gamma \to \pi^+\ \pi^-\ \pi^0\ \ \pi^0$ with 2 undetected charged pions. Here we again assume a Poisson distribution for the multiplicity and we compute the probability to obtain a 4 pions state. Since the OPAL detection efficiency for charged tracks is better than 97%, the probability to miss both charged pions is 0.1%. We will strongly overestimate the background by assuming that all the states with $W_{\gamma\gamma}$ above M_R are contributing to the $\pi^+\ \pi^-\ \pi^0\ \pi^0$ final state where $M(\pi^0\ \pi^0) = M_R$ and the charged pions are unseen. Again as can be seen from Table IV this source of background can be neglected. Other possible background such as $e^+\ e^- \to \tau^+\ \tau^-$ where only $2\pi^0$ faking 2γ are detected (i.e. we miss the charged tracks), can be safely neglected.

VI. The Pseudo-Goldstone boson

As an example we study the pseudo-Goldstone boson X^0, considering nearby compositeness [6] where it is expected to decay mainly into 2γ. In fig. 10. are shown the $X^0\gamma\gamma$ coupling for an elementary and a composite X^0 .

The width $X^0 \to \gamma\gamma$ is mass dependent and is given by the formula :

$$\frac{\Gamma_{(X^\circ \to \gamma\gamma)}}{M^3_{X^\circ}} = \frac{4}{3}\,\frac{\Gamma_{(Z \to e^+e^-)}}{M^3_Z} = 0.16 \quad \frac{keV}{GeV^3}$$

From this expression one obtains that $\Gamma_{\gamma\gamma}$ = 1.3, 4.3, 10 and 20 MeV for the masses M_{X° = 20, 30, 40 and 50 GeV respectively. Our results for the X° signal are given in Table V together with the background which is copied from Table III.

Table V

No. of Pseudo-Goldstone bosons events in $\gamma\gamma$ collisions
and the expected background events from table III.

M_R (GeV)	$\Gamma_{X^\circ \to \gamma\gamma}$ (GeV)	W_{vis} range (GeV)	Efficiency	# events	# BG events from radiative $\gamma\gamma$	s.d.
20	$1.3\ 10^{-3}$	16-24	0.935	$1.2\ 10^4$	$8.6\ 10^3$	129
30	$4.3\ 10^{-3}$	26-32	0.893	$6.9\ 10^3$	$6.5\ 10^3$	87
40	$1.0\ 10^{-2}$	36-42	0.860	$4.3\ 10^3$	$5.7\ 10^3$	58
50	$2.0\ 10^{-2}$	46-52	0.833	$2.7\ 10^3$	$4.9\ 10^3$	43

From this table one can in principle deduce the minimum $\Gamma_{\gamma\gamma}$ value which will result in a resonance of more than 5 standard deviations above background. In the case of M_R = 50 GeV, this minimum is $\Gamma_{\gamma\gamma}$ = 1 MeV.

VII. Conclusion

This study has shown that the production of standard Higgs in a 2γ collision is undetectable. This fact can be used as a support for identification of standard Higgs candidates. On the other hand there is a good chance to see any J=0 resonances having a mass between 20 and 50 GeV and $\Gamma_{\gamma\gamma}$ width of the order of ~ 10 MeV which have a dominant decay either to 2 jets or to 2γ. To this class of particles

belongs the non-standard Higgs and the pseudo- Goldstone boson, even if its $\Gamma_{\gamma\gamma}$ is as low as ~ 1 MeV. Finally one should note that most of the background estimates used here were very conservative and it is not excluded that resonances with $\Gamma_{\gamma\gamma}$ even lower than 1 MeV can still be measured in the 2γ decay mode.

References

1) A. Poppe, Int. Journal of Mod. Phys. A1 (1986) 545

2) G. Alexander, A. Fridman, La Rivista del Nuovo Cimento, 4 (1981) 1

3) F.C. Erne, Proc. of the ECFA-Workshop LEP200,Aachen 86, CERN 87-08, ECFA 87/108 (1987) p.211
F.M. Renard, Phys.Lett. 126B (83) 59
U. Baur, H. Fritzsch and H. Faissner, Phys.Lett. 135B (84) 313

4) T. Sjöstrand, LUTP 85-10 (October 85)

5) J. Ellis, M.K. Gaillard,D.V. Nanopoulos, Nucl. Phys. B106 (1976) 292, see also L.B. Okun, Leptons and Quarks, North-Holland publishing company, 1982. which expresses $\Gamma(H \rightarrow \gamma\gamma)$ as a function of the intermediate virtual particle mass m_V. For m_H = 50 GeV and m_V = 80 GeV one obtains $\Gamma_{\gamma\gamma}$ = 0.7 keV, the same value obtained by J.Ellis et al.

6) F. Shrempp, DESY 85-006 (January 85)

7) V.M. Budnev et al. Phys. Reports 15C (75) 181

8) G. Alexander, U. Maor, C. Milstène, Phys. Lett. 131B (1983) 224
G. Alexander, Invited talk, Proc. of the VII Int. Workshop in $\gamma\gamma$ collisions, Paris, April 1/5/86, p.142

9) A. Berhends and R. Kleiss, Nucl. Phys. 186 (1981) 22

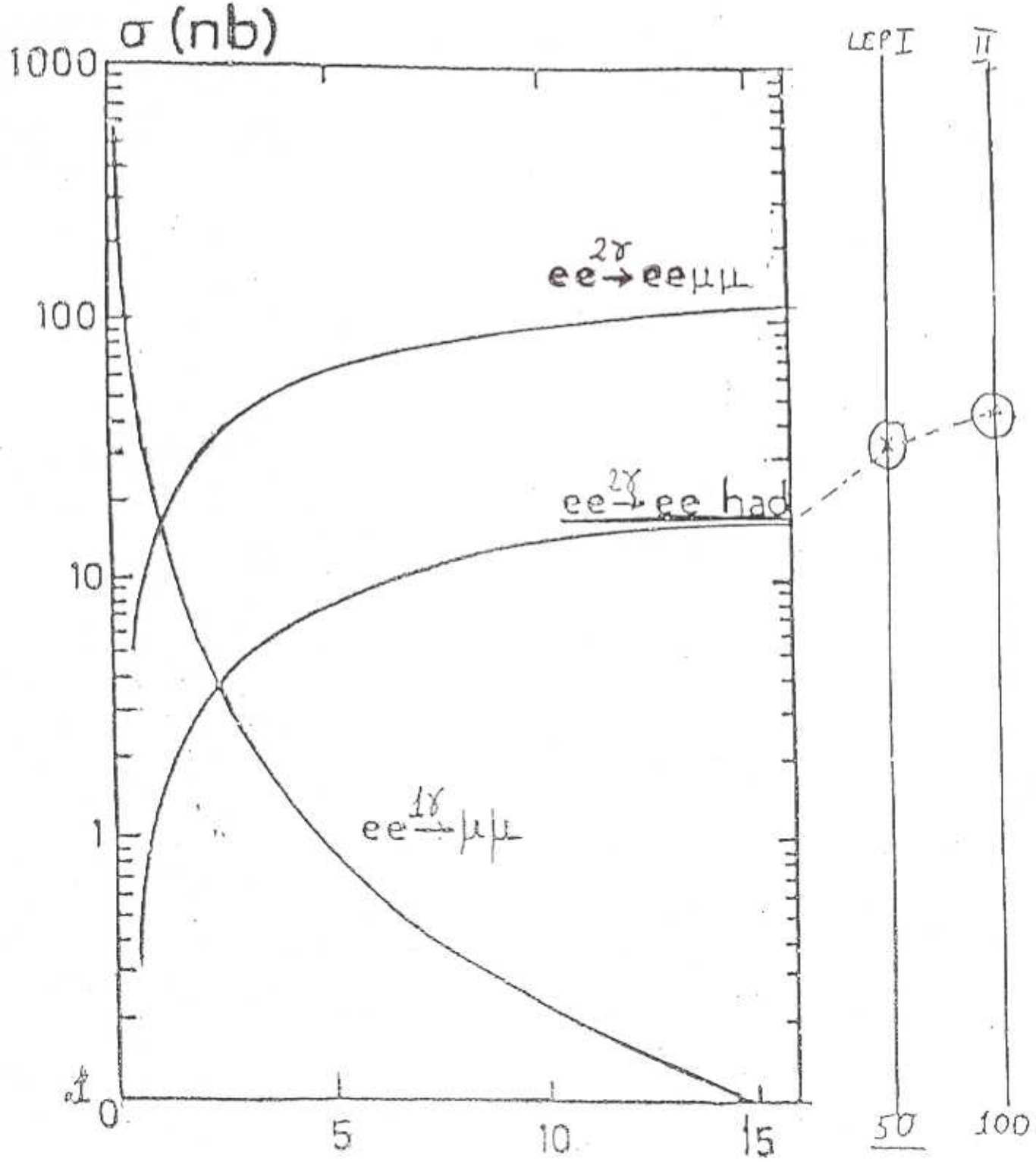

Fig. 1

$E_{beam} = E_{cm}/2$ (GeV)

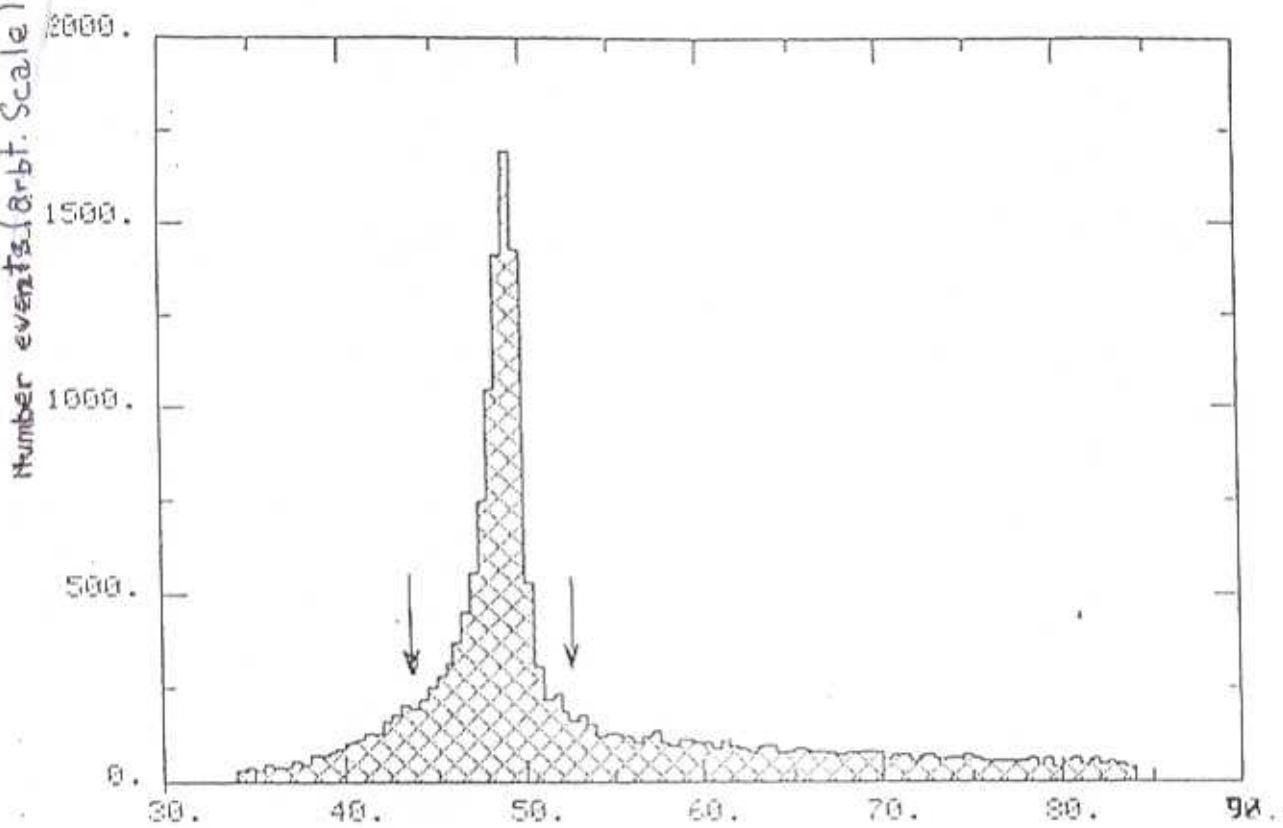

WUIS

Fig. 2

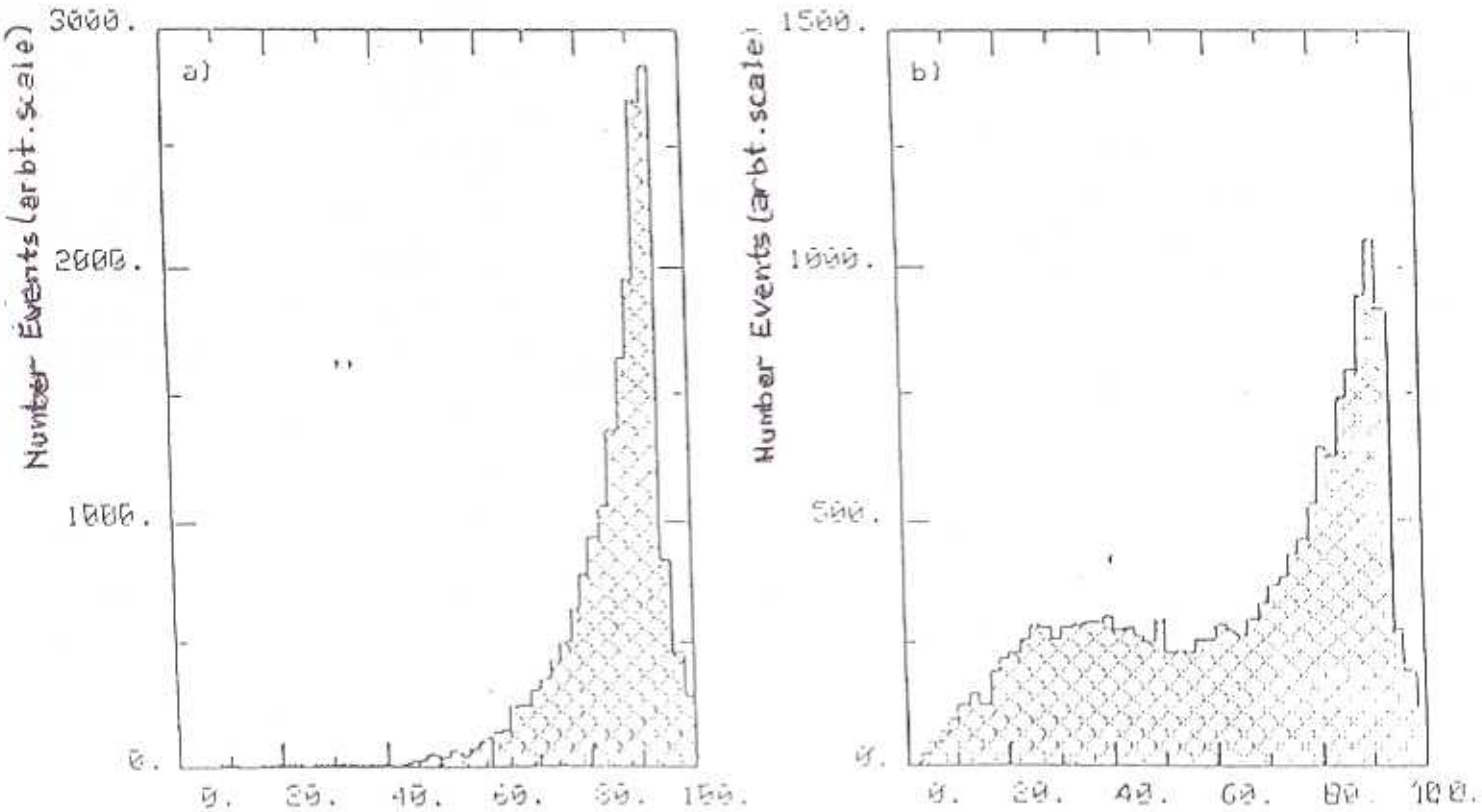

Wuis Fig. 3 Wuis

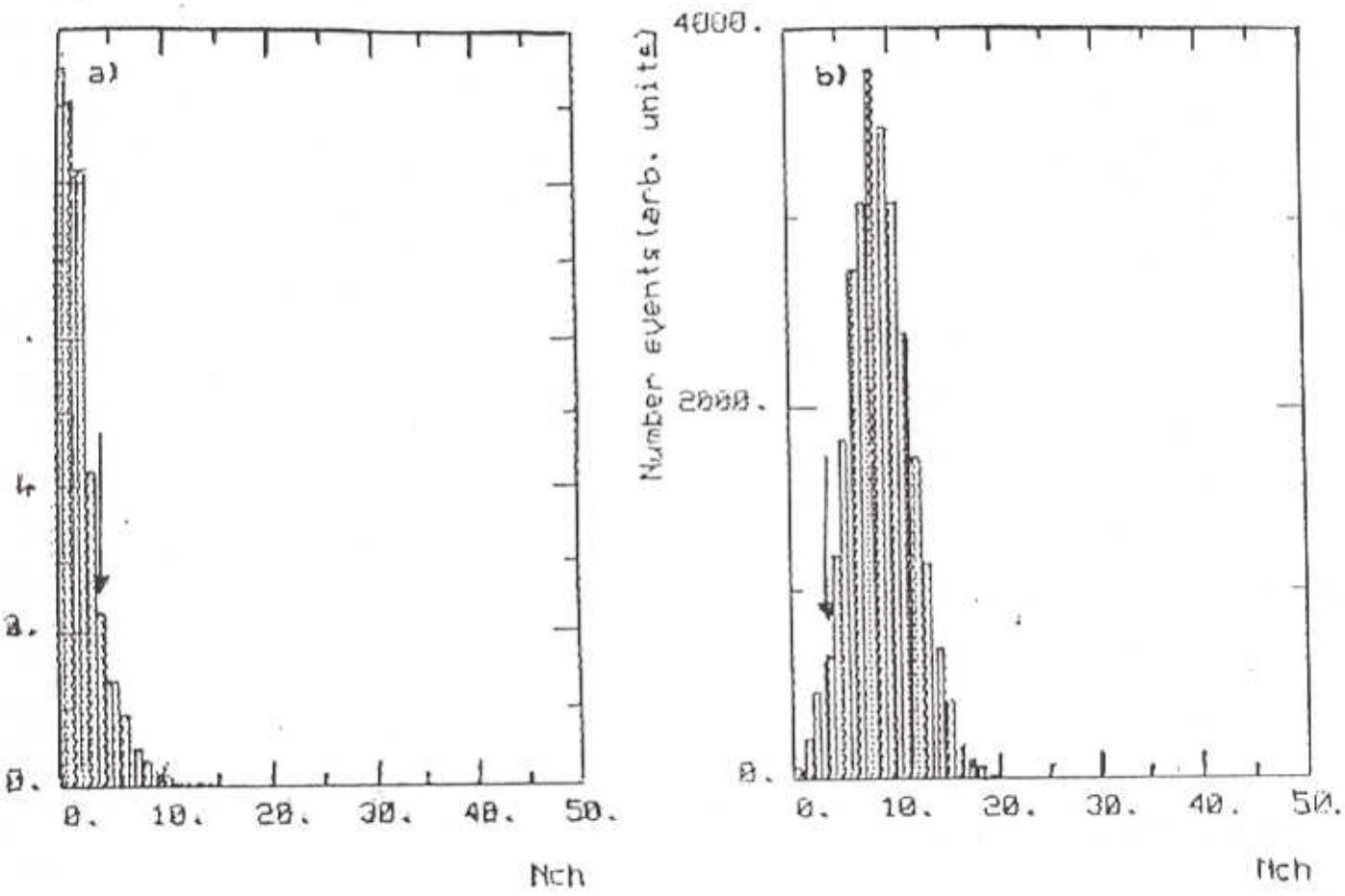

Fig. 4

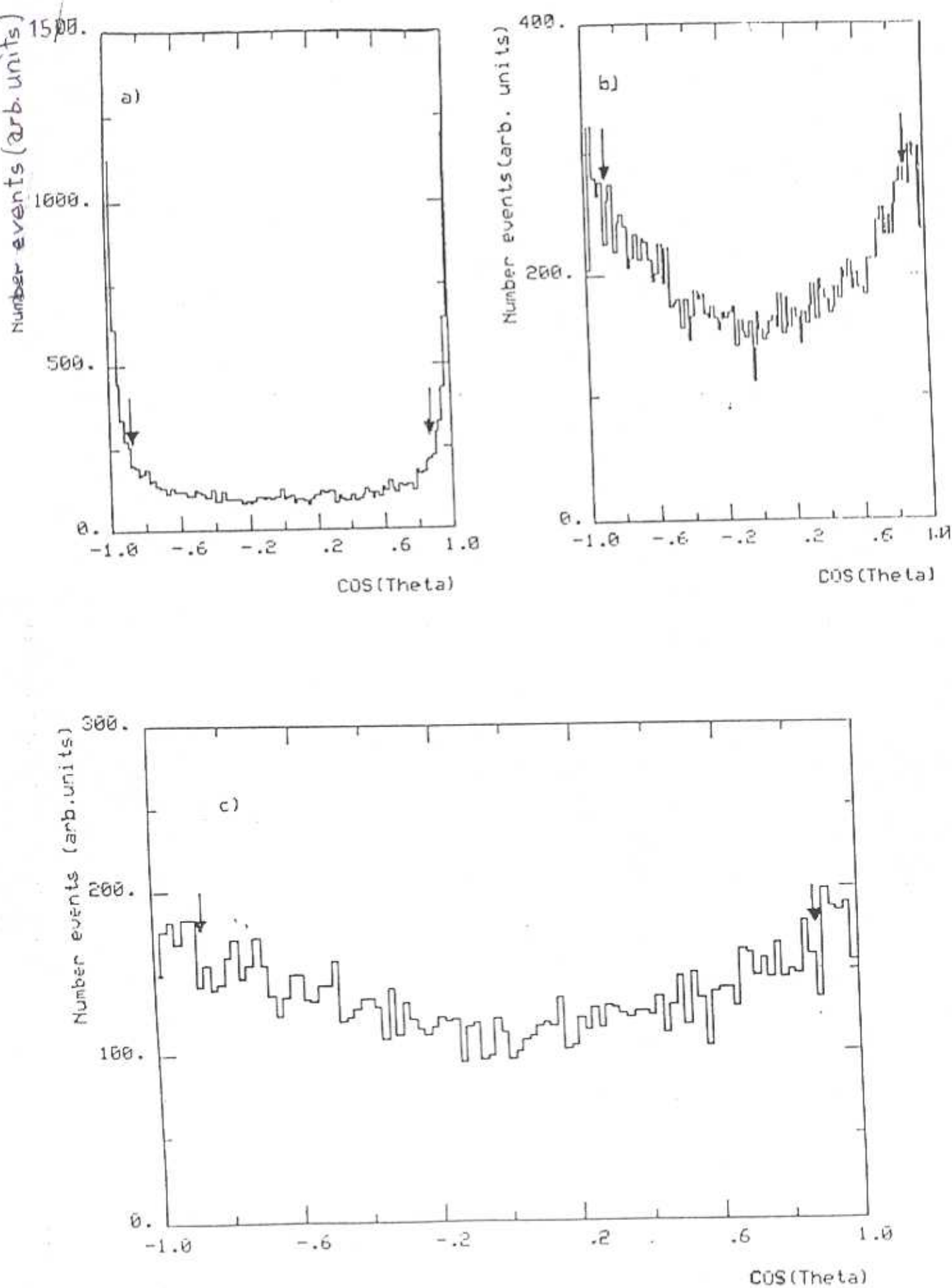
a)
Number events (arb. units)
1500.
1000.
500.
0.
-1.0
-.6
-.2
.2
.6
1.0
COS(Theta)
b)
Number events(arb. units)
400.
200.
0.
-1.0
-.6
-.2
.2
.6
1.0
COS(Theta)
c)
Number events (arb.units)
300.
200.
100.
0.
-1.0
-.6
-.2
.2
.6
1.0
COS(Theta)

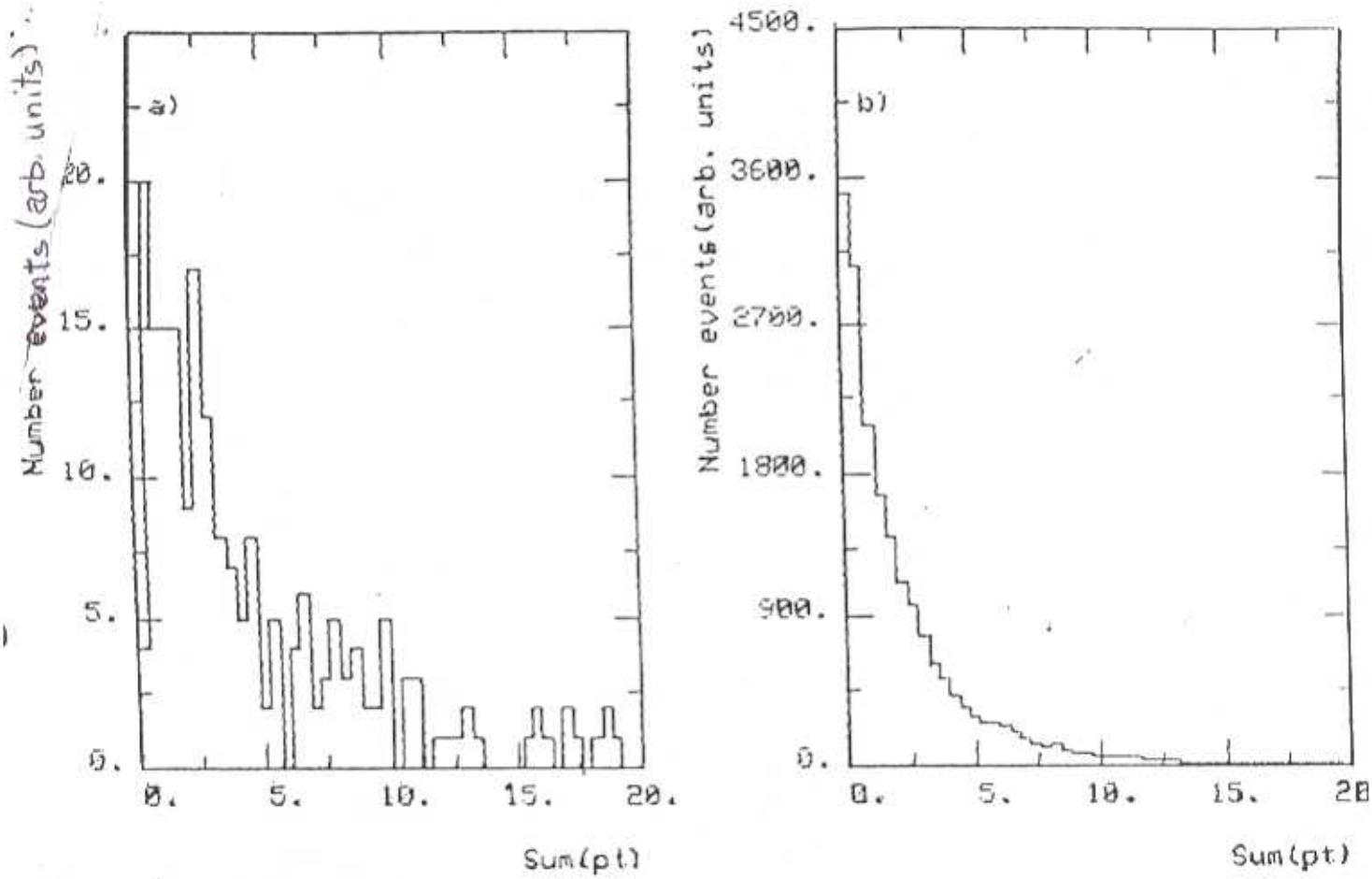
a)
Number events (arb. units)
20.
15.
10.
5.
0.
0.
5.
10.
15.
20.
Sum(pt)
b)
Number events (arb. units)
4500.
3600.
2700.
1800.
900.
0.
0.
5.
10.
15.
20
Sum(pt)

Fig. 6

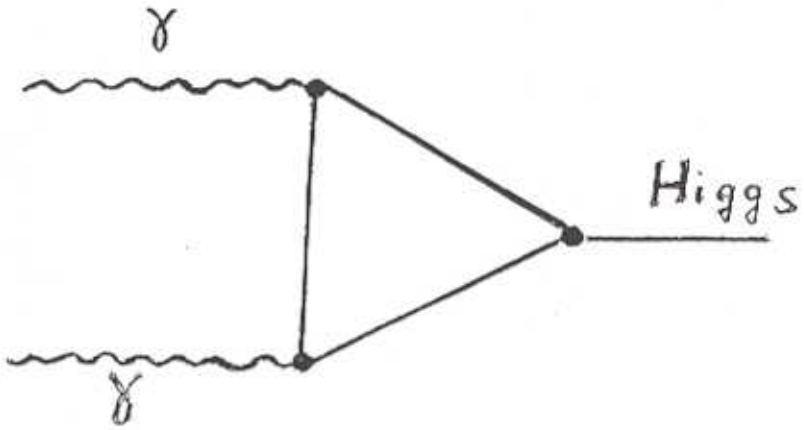
γ
Higgs
γ

Fig. 7

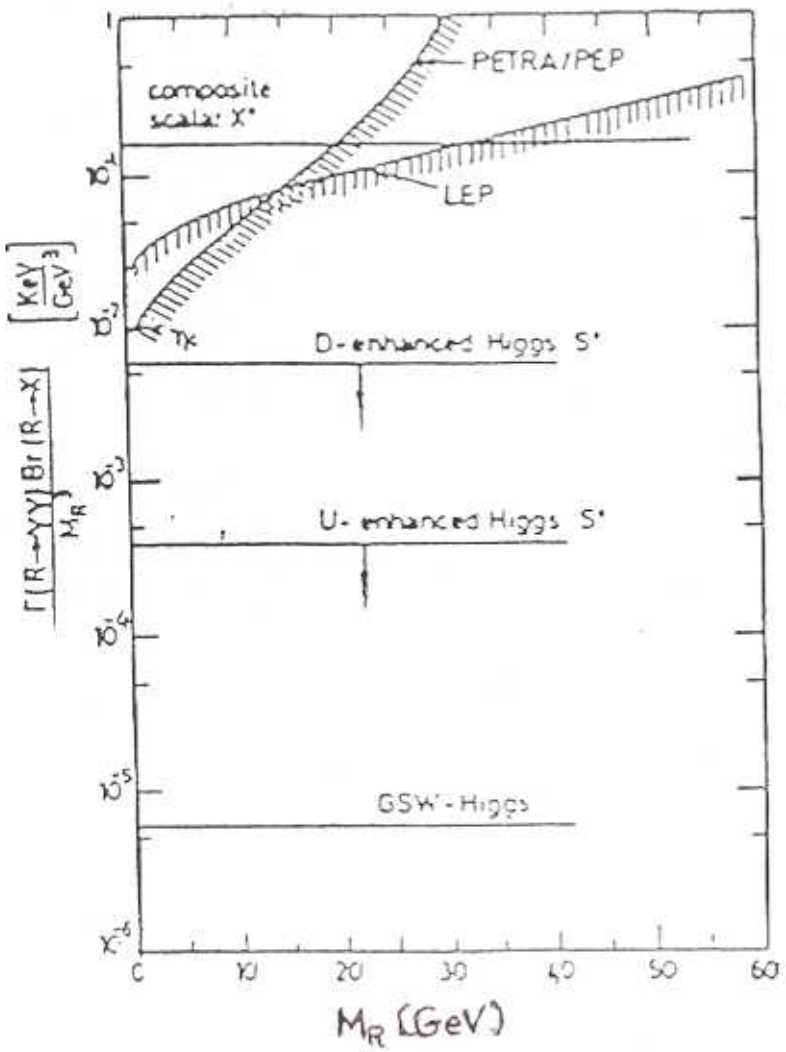
composite scalar X*
PETRA/PEP
LEP
D-enhanced Higgs S*
U-enhanced Higgs S*
GSW-Higgs
$\frac{\Gamma(R\to\gamma\gamma)\,Br(R\to X)}{M_R}$ $\left[\frac{KeV}{GeV^3}\right]$
0
10
20
30
40
50
60
M_R [GeV]

Fig. 8

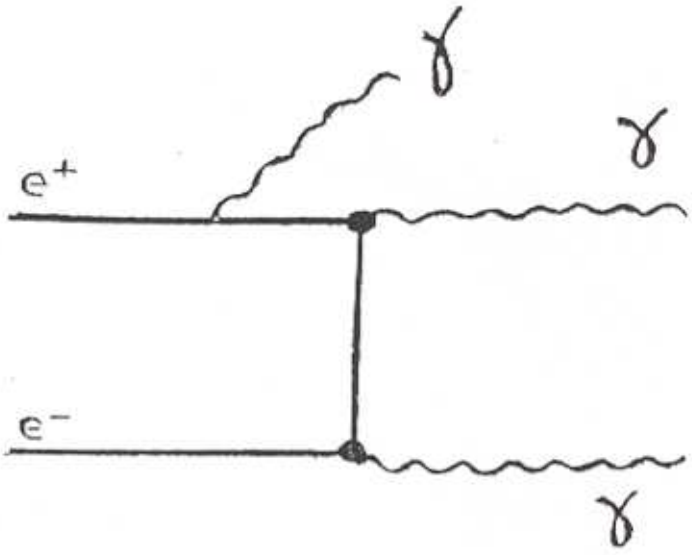

Fig. 9

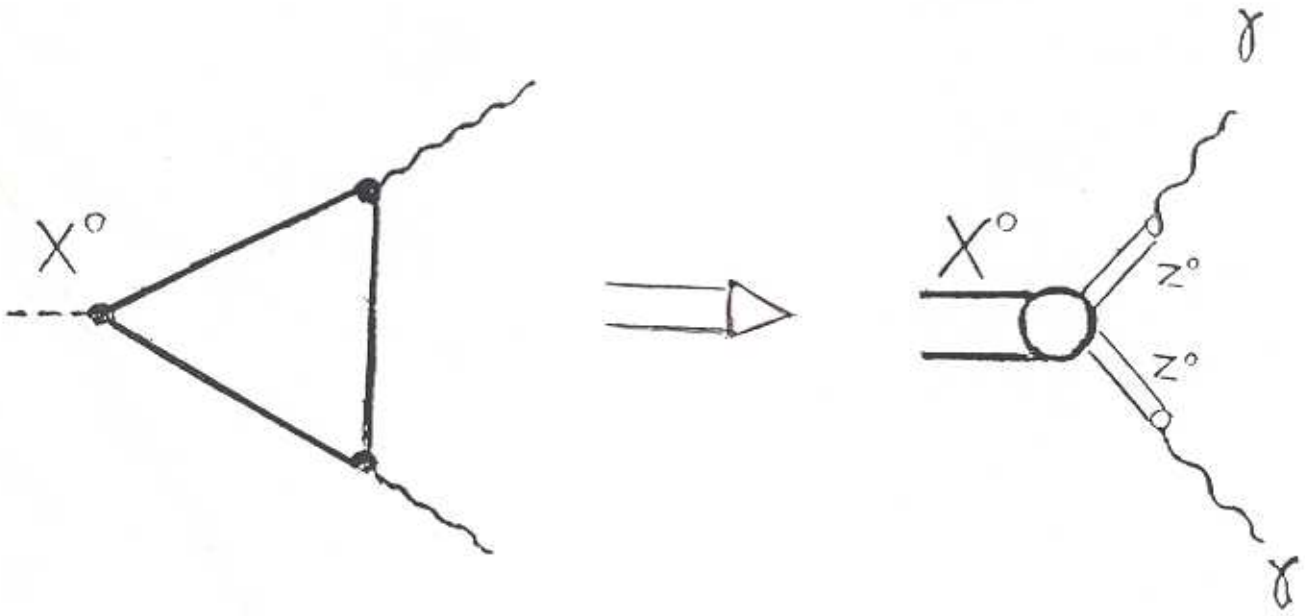

Fig. 10